RSC Advances

ROYAL SOCIETY OF CHEMISTRY

www.rsc.org/advances

Journal Name

Dual Redox-Triggered shell-sheddable micelles self-assembled from mPEGylated starch conjugates for rapid drug release

Mingjia Chen, Chunmei Gao, Shaoyu Lü, Yuanmou Chen, and Mingzhu Liu*

Received 00th January 20xx,
Accepted 00th January 20xx

DOI: 10.1039/x0xx00000x

www.rsc.org/

At present, diselenide bonds have been considered as a novel dual redox-sensitive linkage. Nevertheless, rare studies have focused on diselenide-linked polysaccharide as new biological materials. In this work, the diselenide-linked mPEGylated starch amphiphilic polymer (mPEG–SeSe–St), which combined the biocompatibility of polysaccharide and the stimuli-responsiveness of diselenide linkages, was developed as a novel type of PEG-detachable drug vector for rapid drug release. The amphiphilic design of the mPEG–SeSe–St enabled the formation of self-assembled micelles with spherical core–shell structures in aqueous solution. The data of well-ordered appraisals demonstrated that mPEG–SeSe–St could be disrupted in the presence of low concentration of hydrogen peroxide (H_2O_2, 0.1% (v/v)) or glutathione (GSH, 1 mM). The process of diselenide bonds more rapid degradation than disulfide bonds led to a synergistically enhanced release of loaded anticancer drugs (DOX) in cellular environments. These results, combined with cell viability measurements and confocal laser scanning microscopy (CLSM), indicated that mPEG–SeSe–St micelles might have appeared as a refined platform for cancer therapy.

Introduction

In addition to standard formulation techniques, polymeric micelles, an important nanocarrier focused on enhancing pharmaceutical bioavailability, may be used for solubilization, stabilization, and delivery of challenging agents. The functional properties of micelles based on amphiphilic polymers render them ideal for encapsulation and delivery of anticancer drugs. In aqueous solution, Amphiphilic block copolymers self-assemble to form micelles based on hydrophilic/hydrophobic different ratio in the block copolymer. [1-4] The hydrophobic inner core acts as a warehouse for drugs and the hydrophilic outer shell as a protective interface between the hydrophobic core and the external aqueous circumstance.[5, 6] Typical examples of these polymeric micellar systems have been reported such as micelles based on poly(ε-caprolactone),[7, 8] polylactide,[9, 10] and polystyrene blocks.[11, 12]

As alternatives to traditional micelle systems, intelligent nanocarriers are actively chosen that can stably encapsulate therapeutics and release them at a desired site in response to external stimuli such as pH, redox, glucose and enzyme conditions.[13] Cancer cells exhibit redox rich surroundings due to high cytoplasmic concentration of reducing agents such as glutathione (GSH). Glutathione, a thiol-containing tripeptide that cleaves disulfide bonds via redox reaction,[14, 15] is substantially 1000-fold higher than the level in the blood plasma.[16] Selenium (Se) is a basic trace element for growth, development, metabolism, antioxidant defense system and immune function in human beings.[17-19] Chalcogen sulfur and selenium are analogous in many elements, Containing electronegativity, atom size, and available oxidation states.[20] Particularly, the electronegativity of selenium is weaker than that of sulfur, while the radius of the selenium atom is larger than that of sulfur. This leads to higher bond energy of disulfide than diselenide, which implies that diselenide bonds are more readily cleaved than disulfide bonds.[21, 22] Xu and Zhang and co-workers [21, 23-27] first synthesized a series of dual-redox-responsive diselenide-containing multi-cleavable polymer micelles and studied their redox-responsive disassembly via addition of reductants or oxidants, which boosted the release of encapsulated molecules. Jin et al.[28] reported amphiphilic diblock polymer micelles labeled with a single diselenide with potential application in drug delivery. Wang et al.[22] reported a novel type of PEG-detachable polycation using diselenide bonds to obtain efficient gene carriage with minimal toxicity. However, rare studies have focused on diselenide-linked polysaccharide for drug delivery to address the problematical challenge of wonderful extracellular stability and admirable intracellular cargo release capability.

Natural polysaccharides, including dextran, chitosan, curdlan[29] and starch,[30] appeal to much attention due to their bountiful resource, favorable biocompatibility, innocuity to human bodies of their products. A large number of studies have been reported to research and characterize the features

State Key Laboratory of Applied Organic Chemistry, Key Laboratory of Nonferrous Metal Chemistry and Resources Utilization of Gansu Province and Department of Chemistry, Lanzhou University, Lanzhou 730000, PR China. E-mail: mzliu@lzu.edu.cn; Fax: +86-931-8912582; Tel: +86-931-8912387

† Electronic Supplementary Information (ESI) available: ^{1}H NMR spectrum of DSeDPA, FTIR spectra of starch and mPEG-SeSe-St and the DSC curves of starch and mPEG-SeSe-St.
See DOI: 10.1039/x0xx00000x

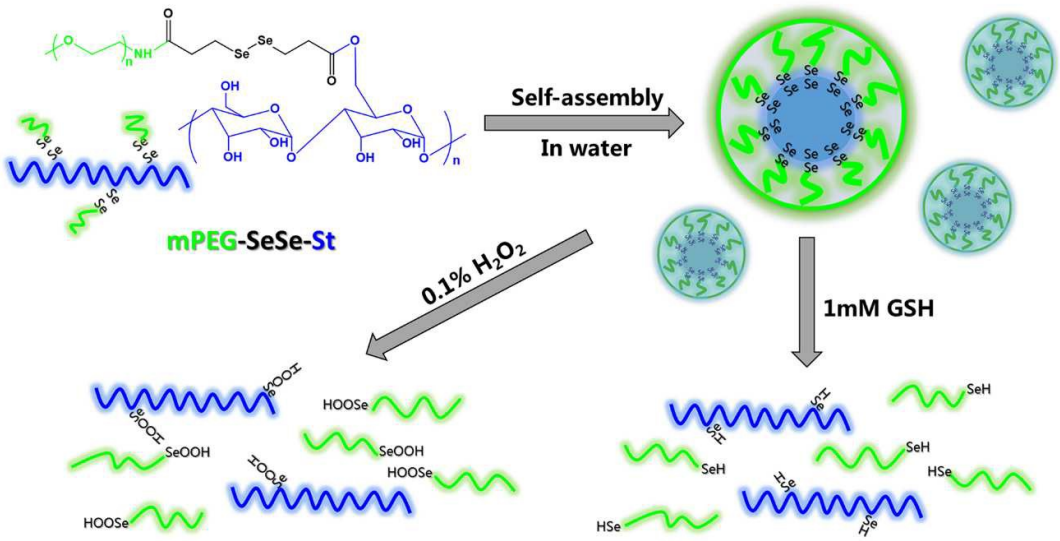

Scheme 1 Schematic of the oxidation and reduction responsive transformation of mPEG-SeSe-St micelles.

of polysaccharide copolymers, particularly developing their favorable potential for medical application and biotechnology.[31] Starch, a significant class of natural polysaccharides, is a fascinating option for other chemically synthesized polymers because of its non-immunogenicity, non-toxicity, compatibility with many drugs and stableness in the air.[32, 33] Compared with other polysaccharides, starch has the extra advantages of a high cost performance and biodegradability not only by hydrolysis, but also by human enzymes, particularly α-amylase.[34] What is more, the existence of amylase-producing tumors has been reported,[35, 36] which could be also a good target for α-amylase degradable starch-based delivery systems. Besides, starch is suitable for assisting chemical modifications to achieve multifarious anticipated functional materials owing to the a mass of functional hydroxyl groups with the chains.[37, 38] As a result, thanks to their excellent advantages, hydrophobic starch derivatives, such as propyl starch[38] and palmitoylated starch acetate,[39] have been prepared and investigated their capacity to encapsulate anticancer drugs and apply in delivery systems.

In this study, diselenide bonds were introduced between mPEG and starch to develop a novel redox-responsive amphiphilic polymeric micelles (mPEG-SeSe-St). It was reported that nanocarriers display a prolonged blood circulation by formulated with hydrophilic neutral surface coatings.[40-42] mPEG, because of its non-immunogenicity, promising biocompatibility and admirable water solubility, was selected as a hydrophilic outer shell. mPEG-SeSe-St was synthesized by stepwise coupling reactions of equimolar ratios of methoxypolyoxy-ethylene amine (mPEG–NH_2) with 3,3'-diselenodipropionic acid (DSeDPA) and finally grafted onto the starch backbones. As illustrated in Scheme 1, mPEG-SeSe-St, consisting of starch as the hydrophobic inner core and mPEG as the hydrophilic outer shell, was able to form spherical micelles in aqueous solution. It was anticipated that the diselenide bonds would go through a structural dissociation and rapid drug release from micelles once treatment with oxidants or reductant.

The physicochemical properties of mPEG-SeSe-St were characterized by FTIR, ^{1}H NMR, X-ray diffraction (XRD) and differential scanning calorimetry (DSC). The mPEG-SeSe-St micelles were prepared and characterized by fluorescence techniques, dynamic light scattering (DLS) and transmission electron microscopy (TEM). Furthermore, their redox-sensitive drug release behaviors and Cell viability were tested, then the intracellular release of DOX was investigated using confocal laser scanning microscopy (CLSM).

Materials and methods

Materials

Soluble starch (Mw=8.8 kDa) was purchased from Zhejiang Linghu Chemical Reagent Factory (Zhejiang, China). Selenium powder, sodium borohydride ($NaBH_4$), 3-chloropropionic acid, N-hydroxy succinimide (NHS), N,N'-dicyclohexylcarbodiimide (DCC), 1-Ethyl-3-(3-dimethylaminopropyl) carbodiimide hydrochloride (EDC•HCl), and Methoxypolyethylene glycol (mPEG–OH, 1.9 kDa), were obtained from Aladdin (Shanghai, China). 4-Dimethylaminopyridine (DMAP) was purchased from Sinopharm Chemical Reagent Co.,Ltd. Doxorubicin hydrochloride (DOX•HCl) and GSH (a reduced form) were purchased from LSB Biotechnology Inc. (Xi'an, China). Methanesulfonyl chloridewas (MsCl) was purchased from SanYou Reagent Factory (Shanghai, China). Pyrene was purchased from Sigma-Aldrich. The other reagents were of analytical grade and used without further purification.

Synthesis of Methoxypolyethylene glycol amine (mPEG–NH_2)

Methoxypolyethylene glycol amine (mPEG–NH_2) was prepared imitating reported procedure.[43] In brief, 5g of Methoxypolyethylene glycol 1900 was dissolved in 75 mL of dry CH_2Cl_2. 4.2mL of triethylamine was added, and 1.2 mL of MsCl was added dropwise with stirring in an ice water bath.

The ice bath was removed, when the MsCl was completely added. The reaction was stirred overnight at room temperature. The reaction mixture was filtered to remove insoluble by-products. The resulting product was crystallized and washed with Et_2O by 3 times to give the light yellow mPEG–Ms. Subsequently, the mPEG-Ms was dissolved in 100 mL of aqueous Ammonia containing 5% NH_4Cl and The reaction mixture was stirred for 72 h in a sealed flask.Then, the product was extracted 3 times with CH_2Cl_2 and dried by Na_2SO_4. The solvent was removed by the rotary evaporation. The product was crystallized from Et_2O and dried in vacuum. The yield was 60%. ^{1}H NMR ($CDCl_3$) δ (ppm): 3.6 (bs, ~170H, **PEG**1900), 3.3 (s, 3H, -O**CH$_3$**), 2.5 (t, 2H, -**CH$_2$**NH$_2$), 1.9 (s, 2H, -**NH$_2$**).

Synthesis of mPEGylated DSeDPA (mPEG-SeSe)

The diselenide bond-containing linker, DSeDPA, was firstly synthesized according to a previous study with some modifications.[44] Then the mPEGylated DSeDPA(mPEG-SeSe) was synthesized using the published procedure.[22] Briefly, 1.1 equivalent of DSeDPA was dissolved in 15 mL DMSO under stirring. To activate the carboxyl groups of DSeDPA in the DMSO, equal amounts of DCC (1.2 equiv.) and NHS (1.2 equiv.) were added into DSeDPA solution for 1 h at room temperature under a nitrogen atmosphere. Then mPEG–NH_2 (1 equiv.) was added into the DMSO solution containing DSeDPA. The mixture was reacted under gentle stirring at room temperature for 24 h. The reactant mixture was filtered and crystallized in cold diethyl ether. Subsequently, the crude product was dialyzed against the excess amount of distilled water for 3 days using a dialysis tube (MWCO 1000 Da). Finally, the sample was followed by lyophilization to obtain mPEG-SeSe conjugates.

Synthesis of mPEG-SeSe-starch copolymers (mPEG-SeSe-St)

The mPEG-SeSe-St copolymers were conveniently prepared by conjugating starch with mPEG-SeSe. Typically, 1.2 g starch, 3.2 g mPEG-SeSe, 0.56 g EDC•HCl and 0.018 g DMAP were dissolved in 50.0 mL DMSO under stirring. The mixture was reacted at room temperature for 48 h. Then, the mixture was purified in a dialysis bag (MWCO 7000 Da) against deionized water for 3 days to remove the solvent and by-products. The solution was lyophilized to achieve the product mPEG-SeSe-St as a light yellow solid (yield: 75.3%). Similarly, mPEG–SS–St was synthesized by the above processes using 2, 2'-dithiodipropionic acid as cross linkers.

Characterization of mPEG-SeSe-St

The chemical structure of mPEG-SeSe-St polymers was confirmed using ^{1}H NMR (Bruker Avance III 400, DMSO-d6) and a Fourier transform infrared (FTIR) spectrometer (Nicolet 670 FTIR, USA).

X-ray diffraction (XRD) spectrometry was obtained from an X-ray diffractometer (Shimadzu XRD-6000) using CuKα radiation (tube operating at 40 kV and 40 mA). Diffractograms were obtained from 2θ= 2–60° with a continuous scan mode to collect data.

The thermal analysis of starch and mPEG-SeSe-St polymers were measured on differential scanning calorimetry (DSC) (Perkin-Elmer Corp., Wilton, CT). A total of 3 mg samples sealed in an aluminium pan were heated from 20 to 220 ^{o}C with a heating rate of 10 ^{o}C /min under nitrogen atmosphere.

Preparation and characterization of micelles

Preparation of mPEG-SeSe-St micelles

25 mg of mPEG-SeSe-St polymers were dissolved in 25 mL of phosphate buffered saline (PBS) solution under gentle shaking at 25 ^{o}C for 4 h, followed by sonication using an ultrasonicator (KQ-400KDE, KunShan Ultrasonic instrument Co., Ltd., China) for 10 min at 100 W. The resulting micellar solution was passed through a 0.45 μm filter (Millipore) and stored at room temperature.

Characterization of mPEG-SeSe-St micelles

The critical aggregation concentration (CAC) of amphiphilic mPEG-SeSe-St micelles were estimated by fluorescence spectroscopy technique (LS55, Perkin–Elmer, America), using pyrene as a hydrophobic probe. Briefly, 1 mL of 6.0×10^{-8} M pyrene solution in acetone was added to a series of colorimetric cylinder (10 mL) and then acetone was removed by evaporation. 10 mL of various concentrations of mPEG-SeSe-St polymers solutions (1–4×10^{-5} mg/mL) were added to the colorimetric cylinder and sonicated for 2 h to reach the solubilization equilibrium of pyrene between water phase and micelles. Then the samples were put overnight at room temperature. The excitation spectra of pyrene were recorded using a fluorescence spectrophotometer with an emission wavelength (λ_{em}=390 nm) and the slit-widths of both excitation and emission was 15 nm. The fluorescence spectra were obtained at λ_{max}=330 nm.

Polymeric nanoparticles were determined using Zetasizer Nano ZS (DLS) on a 90 Plus particle size analyzer (Brookhaven Instruments Corporation) at room temperature. All sample solutions were filtered by the 0.45 μm filter (Millipore) and analyzed at a fixed angle of 90^o for duration of ~10 min in triplicate at the concentration of 1.0 mg/mL. The size and morphology distribution were observed by transmission electron microscopy (TEM, JEM-1200EX/S, Hitachi, Japan) operated at an accelerating voltage of 200 kV. The micellar suspension were deposited onto copper TEM grids (400 mesh, carbon coated), blotted, and then followed by air drying at room temperature.

Disassembly of micelles triggered by GSH and H_2O_2

The mPEG-SeSe-St micelles were prepared as described above and incubated with 1 mM GSH or 0.1% (v/v) H_2O_2 for 1 h, 4 h and 24 h, respectively. The GSH or H_2O_2 was prepared in 0.1 mM HEPES buffer solution (pH 7.4). The size distribution and morphology changes of mPEG-SeSe-St micelles were observed by DLS and scanning electron microscopes.

Cell viability using MTT assay

In vitro cytotoxicity of mPEG-SeSe-St micelles was evaluated by 3-(4, 5-dimethylthiazol-2-yl)-2, 5-dipheny-ltetrazolium bromide (MTT) assay with TC1 Lung cells. The cells suspension in culture medium (DMEM with 5% penicillin–streptomycin and 10% fetal bovine serum) was seeded onto 96-well plates at a density of 5×10^4 cells per/well in 96-well transparent plate, and incubated at 37 ^{o}C in a humidified atmosphere with 5%

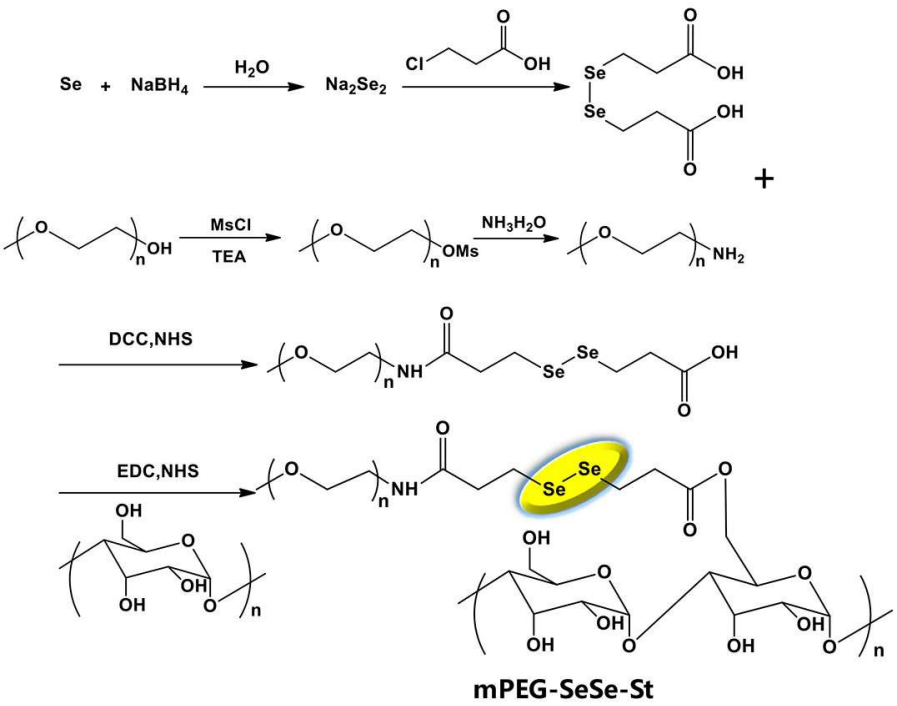

Scheme 2 The synthetic pathway of mPEG-SeSe-St.

CO_2 for 24 h. The cells were then incubated with blank micelles and DOX-loaded micelles for 48 h at 37 °C. The concentration of blank micelles ranged from 5 to 100 μg/mL. DOX-loaded micelles and Free DOX were diluted in complete DMEM at various final DOX concentrations from 0.5 to 10 μg/mL. Afterwards, MTT solution (5 mg/mL in PBS, 20 μL) was added to each well and incubated for another 4 h. The culture medium was removed and 0.15 mL of DMSO was added. The optical density (OD) was measured using a microplate reader (VICTOR 1420, PE, USA) at 490 nm. Cell viability (%) was calculated as (OD of test group/OD of control group) × 100%.

Loading and in vitro redox-responsive release of DOX

DOX-loaded micelles were prepared by dissolving 20 mg polymers (mPEG-SeSe-St and mPEG-SS-St） into DMSO to achieve 5 mg/mL final concentration. Subsequently, 4 mg DOX•HCl and 4.0 equiv. of extra trimethylamine also were dissolved in DMSO with sonicating for 1 h at room temperature and dialyzing against deionized water using a dialysis bag (MWCO 3500 Da) at room temperature until the deionized water outside the dialysis tube demonstrated insignificant fluorescence emission of DOX. Finally, the solution was filtered and lyophilized.

In vitro drug release profiles of DOX-loaded from micelles were studied in PBS (pH 7.4) with or without 10 mM GSH. The 5mg DOX-loaded micelles (mPEG-SeSe-St and mPEG-SS-St） were suspended into the release medium (5mL) and immediately transferred to a dialysis tube (MWCO 3500 Da).The dialysis tube was immersed into 50 mL of corresponding release medium and gently shaken at 37 °C at 100 rpm. At desired time intervals, 7.0 mL of release media was taken out and replenished with an equal volume of fresh medium. The amount of released DOX was determined by fluorescence measurement (481 nm).

Intracellular drug release

TC1 Lung cells seeded at 5×10^4 cells/well into a 96-well black plate and incubated for 24 h in DMEM (2 mL) were treated with DOX-loaded micelles and free DOX (DOX = 15 μg/mL) at 37 °C for 4, 12 and 24 h, respectively. At the same time, blank micelles were used as control. At the designated time interval, cells were washed three times with PBS buffer. After the removal of supernatants, the cells were fixed 4% formaldehyde for 20 min at room temperature. Finally, the cells were stained with 2-(4-amidinophenl)-6-indolecarbamidine (DAPI) and Cellular uptake efficiency were obtained using CLSM (Olympus Fluoview 1000).

Results and discussion

Synthesis and structural analysis of mPEG-SeSe-St

The synthetic pathway was shown in Scheme 2. Firstly, DSeDPA , the diselenide bond-containing linker , was achieved via reacting 3-chloropropanoic acid with Na_2Se_2 and validated by ^{1}H NMR. As revealed in Fig. S1, the peaks at 2.60–2.70 and 2.95–3.05 ppm belonged to the protons of the CH_2CH_2SeSe,[22] which proved that DSeDPA was successfully fabricated. whereafter, the molar ratio of carboxylate groups of DSeDPA to amine groups of mPEG–NH_2 was controlled at 2.2: 1 to acquire carboxyl groups terminated mPEG (mPEG-SeSe). Finally, the mPEG-SeSe-St copolymers were conveniently prepared by grafting mPEG-SeSe onto starch backbone. The chemical structure of mPEG-SeSe-St copolymer

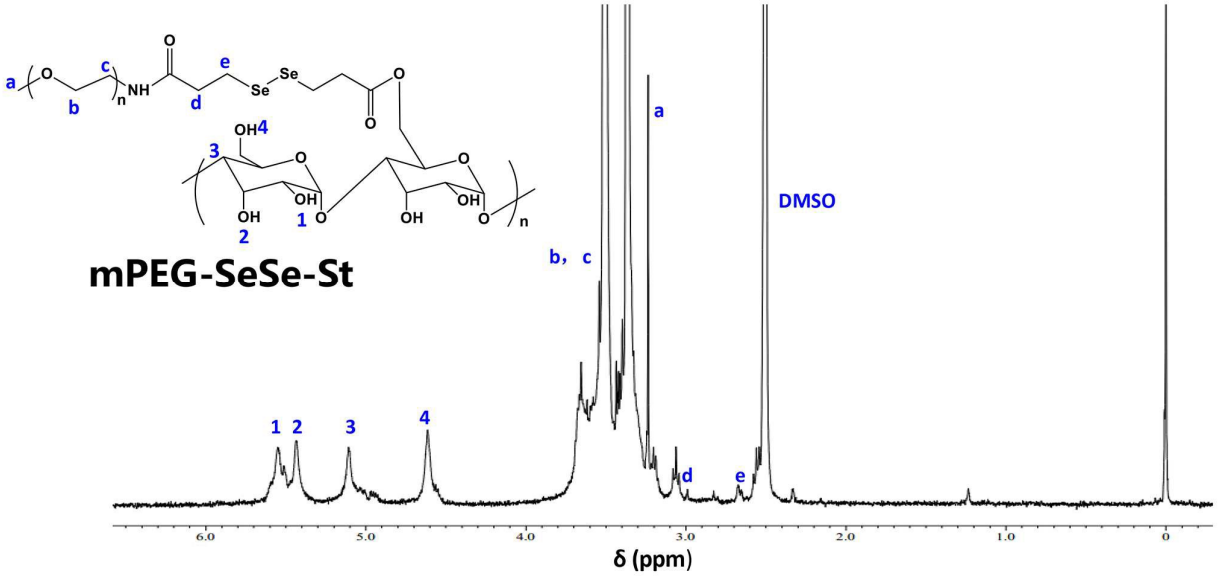

Fig. 1 ^{1}H NMR spectrum of mPEG-SeSe-St in DMSO-d_6.

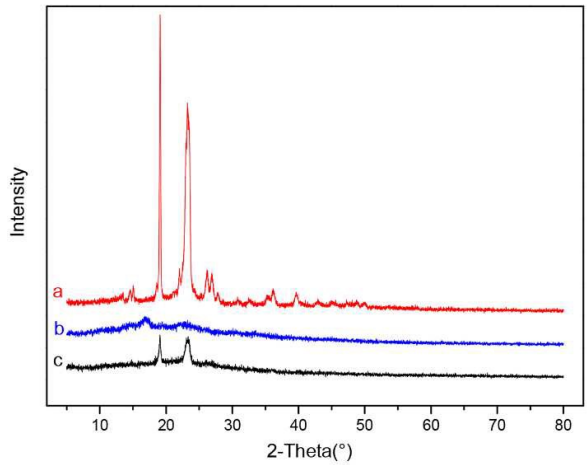

Fig. 2 Wide angle X-ray diffraction patterns of mPEG (a), starch (b) and mPEG-SeSe-St (c).

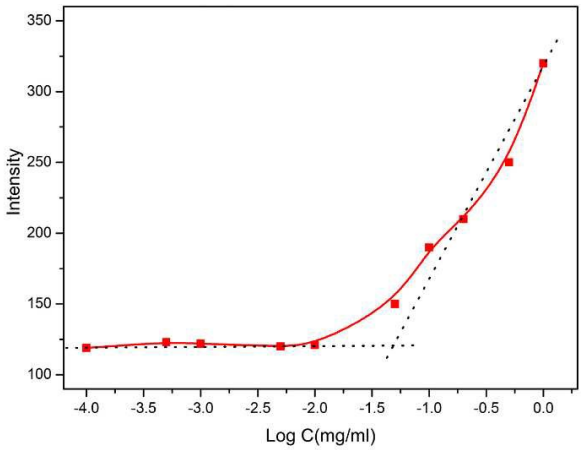

Fig. 3 Intensity (I330) from pyrene excitation spectra as a function of mPEG-SeSe-St concentrations in PBS solution of pH 7.4.

was verified by ^{1}H NMR and FTIR. Fig. 1 displayed the ^{1}H NMR spectrum of mPEG-SeSe-St, in which the representative resonance peaks of both starch and mPEG-NH_2 were clearly shown, expounding the mPEG-SeSe-St conjugates was successfully prepared. Detailedly, the evident four peaks located between 4 and 6 ppm comprising the C2–OH (1, 5.54 ppm), C3–OH (2, 5.43 ppm), C1–H (3, 5.11 ppm) and C6–OH (4, 4.61 ppm) could be apparently ascertained, which were ascribed to the hydroxyl groups from glucose unit of starch.[45] The typical peaks assigned to the methylene protons and terminal methoxyl protons of mPEG were observed at 3.51 ppm (–CH_2–CH_2–, b, c) and 3.23 ppm (–O–CH_3, a). Besides, the characteristic peaks showing at 2.98 ppm (–**CH_2**CH_2SeSe, d) and 2.65 ppm (–CH_2SeSe, e) were ascribed to the the diselenide bond-containing linker (DSeDPA), which could further confirm that the mPEG-SeSe-St was successfully synthesized.

The FTIR spectra also revealed the preparation of mPEG-SeSe-St copolymers, as shown in Fig. S2. A new typical absorption peak appeared at 1104 cm^{-1} (C-O-C stretching vibration) appointed to the ether bond of mPEG, which successfully substantiated the chemical structure of mPEG-SeSe-St copolymers.

To survey the changes of the microstructure between starch and mPEG-SeSe-St conjugate, X-ray diffraction diagrams were determined and the results were shown in Fig. 2. The diffraction curve of mPEG (Fig. 2a) showed several typical crystal peaks at 2θ equals 19.1°, 23.4°, 26.2° and 27.0°. Peaks at 2θ= 17.3°, 22.0°, and 23.9° were the characteristic diffraction of the soluble starch (Fig. 2b) ,which were attribute to the crystal form and also were indicative of the B-type pattern[46]. In contrast of starch, mPEG-SeSe-St conjugates (Fig. 2c) exhibited two diffraction spike at round 2θ= 19.1°, 23.4°, which was assigned to the typical peak of mPEG. However, the characteristic peaks of starch disappeared. The results

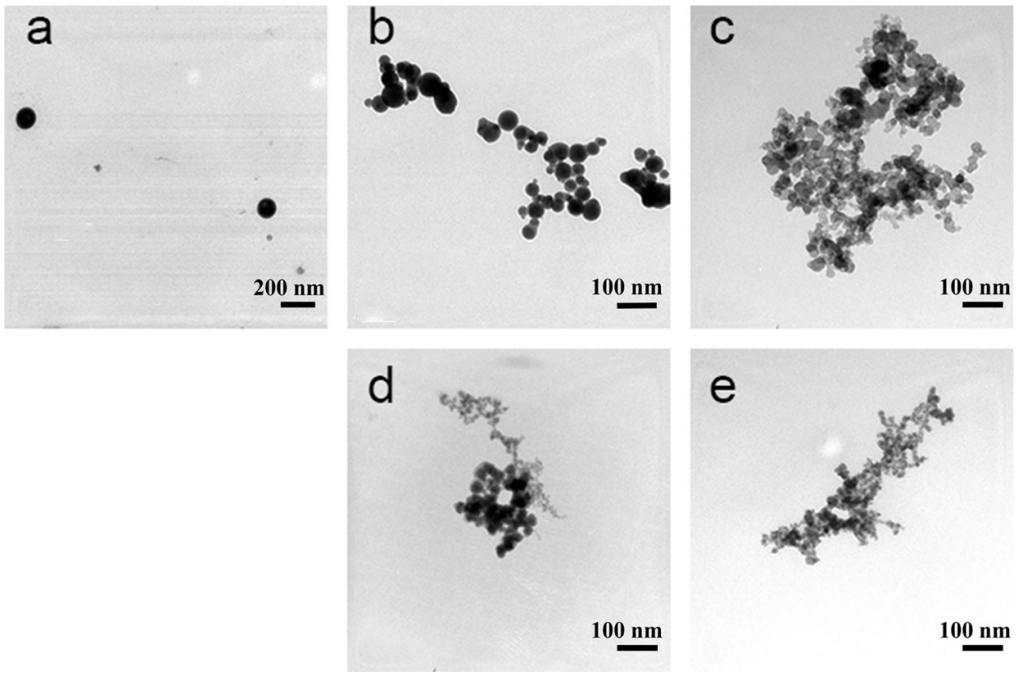

Fig. 4 TEM images of mPEG-SeSe-St polymer micelles (a), oxidized in 0.1% H_2O_2 for 1 h (b) and 24 h (c), reduced in 1 mM GSH for 1 h (d) and 24 h (e).

indicated that the crystalline structure of starch had been completely disturbed after chemically modification with mPEG, further proving that mPEG-SeSe-St was prepared successfully.

DSC thermograms of starch and mPEG-SeSe-St conjugates are presented in Fig. S3. As shown in Fig. S3a, a gelatinization endotherm was detected at 95.7 ^{o}C in starch sample. As examined, the gelatinization endotherm of mPEG-SeSe-St polymers (Fig. S3b) decreased to 50.9 ^{o}C comparing with starch. It was indicative that mPEG affected the starch crystallinity and increased the starch amorphous regions, which eventually led to the decrease of the gelatinization endotherm.

Self-assembly behavior of mPEG-SeSe-St micelles

mPEG-SeSe-St ,composing of hydrophilic mPEG and hydrophobic starch, was a representative amphiphilic polymer which could self-assemble in aqueous solution. During the self-assembly process, the CAC was a vital factor to describe the self-aggregation behavior and also an important parameter in evaluating the stability of micelles in the blood circulation system post-administration.[47-49] The self-assembly behavior of mPEG-SeSe-St polymers in PBS media was examined via the fluorescence probe technique with pyrene as a fluorescence probe. It was shown in Fig. 3 that the intensity (λ = 330 nm) of pyrene ,as a function of polymer concentration ,is rather sensitive to the polarity of microenvironment[50]. It was based on the truth that when pyrene was entrapped in hydrophobic starch core, the fluorescence intensity of pyrene increased, while it was low in water owe to low solubility of pyrene in water. It could be observed that the intensity ratios went through a sudden increase over a certain concentration, while experienced no obvious variation at lower concentrations, indicating the formation of the mPEG-SeSe-St micelles. From Fig. 3, the CAC of mPEG-SeSe-St copolymer was determined to be 0.049 mg/mL.

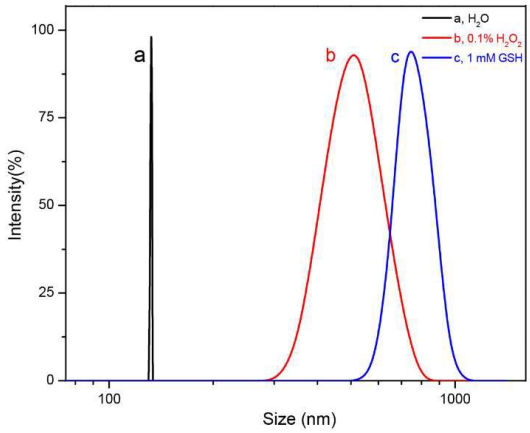

Fig. 5 DLS results of mPEG-SeSe-St polymer micelles in water (a), with H_2O_2 (b) or GSH (c) after 4 h.

Physical characterization of mPEG-SeSe-St micelles and their dual stimuli-responsive property

The polymeric micelles in a size range (<200 nm) could prevent their extravasation into healthy cells as well as reduce renal clearance by kidney filtration and display EPR effect at solid tumor sites for passive targeting.[31, 51-53] The morphology and size of the mPEG-SeSe-St aggregates were examined by TEM and DLS. It was shown in Fig. 4a that the morphology of mPEG-SeSe-St polymeric self-assemblies which formed spherical micelles with a diameter about 123 $\pm$ 4.5 nm. DLS results indicated that the hydrodynamic diameter of $\approx$ 136 nm has a monomodal size distribution (Fig. 5a), which was bigger than that determined by TEM. The difference in micelle sizes between TEM and DLS results could be ascribed to the dried state of the micelles.[54]

It had been reported that hydrophobic diselenide groups could be oxidized to seleninic acid in an oxidizing surroundings and reduced to selenol in the presence of reductants.[21] For that reason, the redox responsive of the mPEG-SeSe-St aggregates was investigated with 0.1% (v/v) H_2O_2 or 1 mM GSH for 1 h, 24 h. The change of micellar aggregates were examined using TEM. The TEM images in Fig. 4b and c displayed that the micellar structure of mPEG-SeSe-St was transformed to atactic aggregates and consolidated to each other to form broad aggregates after oxidized for 1 h, finally to absolute breakdown and aggregation after oxidized for 24 h, reflecting that the oxidation stimulus had actually induced the cleavage of the mPEG-SeSe-St micelles. As shown in Fig. 4 d and e, when 1 mM GSH was added, the complete core–shell structure disassembled and afterward, extra diminutive aggregates shaped after reduced for 24 h, proving that the micellar structures had been ruined by the reducing agent.

The redox responsiveness of the mPEG-SeSe-St micelles was further examined via DLS to image the size of the particles at 0.1% (v/v) H_2O_2 or 1 mM GSH for 4 h (Fig. 5 b and c). After 0.1% (v/v) H_2O_2 treatment, the size of mPEG-SeSe-St micelles showed an markedly increase, from 132 nm to around 526 nm, and with concomitant broadening of the diameter distribution, indicating that the starch chains on the nanomicelles were separated due to the cleavage of the diselenide bonds. Meanwhile, the particle incured a major particle size increase to around 714 nm in presence of 1mM GSH owe to action of GSH on redox responsive diselenide linkages in the nanoparticles resulting in aggregation of hydrophobic starch units causing increase in particle size. However, it was obvious that particle size evaluated from DLS was bigger than that recorded by TEM after treatment with H_2O_2 or GSH. Probably the difference in overall diameters was attributed to that the samples for TEM underwent a shrinkage caused by the water evaporation under air-drying. Moreover, the hydrodynamic diameter analyzed by DLS was the size of the aggregate. Therefore, the micelles suspended in water were bigger than those in dry state in TEM graphs.[55] As demonstrated, such dual redox variation of particle size was caused by the cleavage of diselenide linkages, which led to detachment of the mPEG shells from the micellar nanoparticles and modification of the hydrophilic-hydrophobic balance of the amphiphilic conjugates. This stimulus-induced reordering and degradation of micelles may guarantee the ability of use mPEG-SeSe-St micelles as an ideal intracellular drug-delivery platform.

***In vitro* cell cytotoxicity study**

Cell viability of TC1 Lung cells on treatment with the blank mPEG-SeSe-St micelles was determined by MTT assay. The incubation time was 48 hours and the micelle concentrations were varied from 5 μg/mL to 100 μg/mL. As shown in Fig. 6A, it was clear seen that the cell viabilities of the micelles incubated with TC1 Lung cells were all above 88% at all concentrations from 5-100 μg/mL. It demonstrated that blank mPEG-SeSe-St micelles had a low toxicity and good compatibility to TC1 Lung cells.

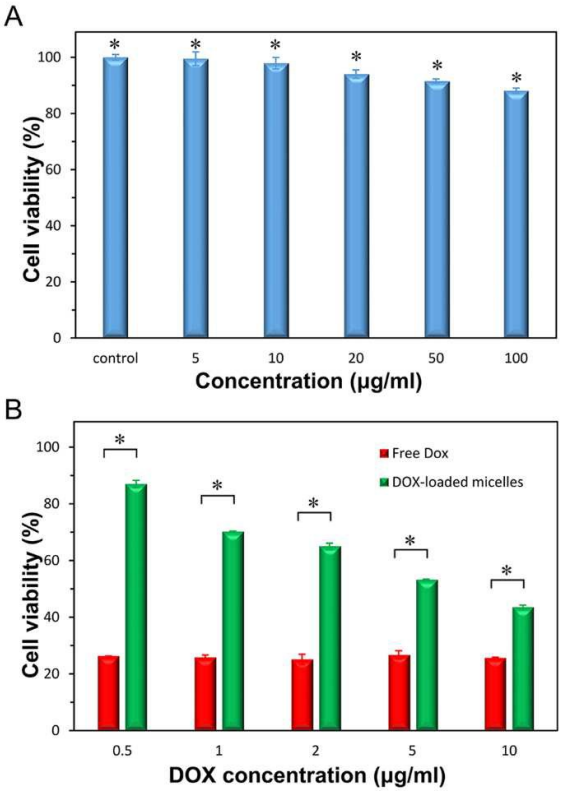

Fig. 6 The viability of TC1 Lung cells after incubation with blank mPEG-SeSe-St micelles (A) and DOX-loaded mPEG-SeSe-St micelles and free DOX (B) at different concentrations for 48 h. Asterisks (*) denote statistically significant differences (*$p < 0.05$) calculated by one-way ANOVA test.

The survivals of TC1 Lung cells treated with DOX-loaded micelles and free DOX were shown in Fig. 6B. Compared with blank micelles, the cell viability extremely decreased and the cytotoxicity increased with the increased concentration of DOX- loaded mPEG-SeSe-St micelles. When the concentration of DOX in mPEG-SeSe-St micelles was 1 μg/ mL, the cell viability was less than 71%. When the concentration was 10 μg/mL, the cell viability decreased to 43%. As a comparison, the cell viability treatment with the free DOX at concentrations from 0.5 to 10 μg/mL was about 25%. This results suggested DOX-loaded mPEG-SeSe-St micelles showed lower activity than the free DOX at the same concentration of DOX. Maybe owe to the time-consuming drug release from the micelles and thus deferred nuclear uptake, the loaded drug in micelles often showed lower activity than the free drug at the same dose.[29]

***In Vitro* drug release and study**

To confirm the practicability of this redox-responsive mPEG-SeSe-St micelles as an intelligent cargo, the anticancer drug DOX was designated and capsulated into the mPEG-SeSe-St micelles, resulting in a pink solution with a definite UV absorption wavelength of 481 nm. The reductive-triggered DOX release behavior was monitored through the increase of UV absorption intensity of the dialysis extracting solution. The drug loading efficiency (DLE) and drug loading content (DLC) of the DOX-loaded micelles are found to be 5.0% and 30.1%, respectively, on the basis of the standard curve of DOX.

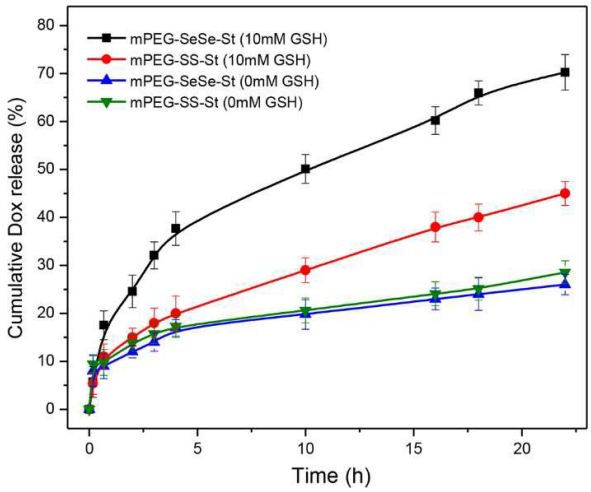

Fig. 7 GSH triggered DOX release profiles from mPEG-SeSe-St micelles and mPEG-SS-St micelles.

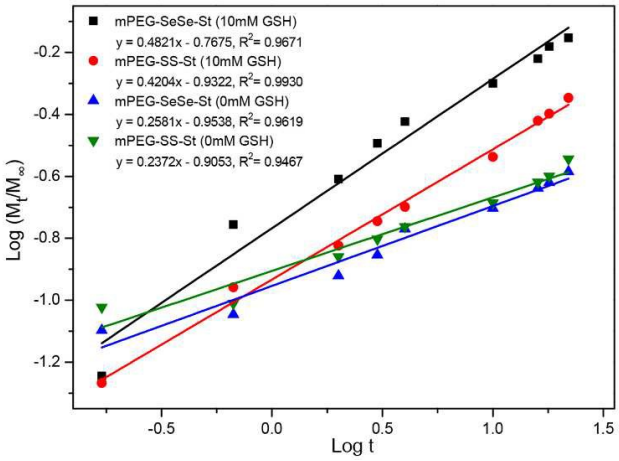

Fig. 8 plots of log (M_t/M_∞) against log t with GSH for DOX in mPEG-SeSe-St micelles and mPEGSS-St micelles.

Similarly, the DOX was loaded into mPEG-SS-St micelles by the same processes. Time-dependent release of DOX from DOX-loaded micelles was performed in buffered solutions (pH 7.4) with or without GSH, mimicking the tumor extracellular microenvironment and blood normal tissues, respectively.

As compared in Fig. 7, minimal drug release (28% and 26%) was observed in mPEG-SS-St and mPEG-SeSe-St DOX-loaded micelles respectively without GSH at 22h. This chiefly met our demand that the drug-loaded micelles would diminish the loss of the trapped load before arriving at the target cells. In presence of 10 mM GSH, accelerated drug release of ~45% and ~70% was observed at mPEG-SS-St and mPEG-SeSe-St DOX-loaded micelles respectively in the same period. This was noticeable that reductive stimulus could accelerate the release of DOX in the site of action though the breakage of the disulfide bonds and diselenide bonds in the polymer backbone. Nevertheless, because of lower bond energy of diselenide than disulfide,[21] diselenide linkage was more sensitive than disulfide linkage at the same concentration of GSH. In comparison with mPEG-SS-St micelles having disulfides in the polymer backbone, the mPEG-SeSe-St having diselenide in the polymer backbone release drug is significantly more rapid. These results are desirable to ensure the predominance of use mPEG-SeSe-St micelles to achieve speedy yet controlled therapeutic delivery in target cells.

The release mechanism studies

It was known that the release mechanism of micelles is a complicated procedure, which may be permeation or diffusion of drugs via polymeric network, the degradation of micelles and the combination of the two circumstances.[37] The classic semi-empirical equation was founded by Ritger and Peppas[56, 57] to confirm drug release mechanism of DOX-loaded mPEG-SS-St and mPEG-SeSe-St.

$$\frac{M_t}{M_\infty} = kt^n$$

$$\log \frac{M_t}{M_\infty} = n \log t + \log k$$

where M_t and M_∞ are the accumulative amount of DOX released at time t and infinite time, respectively; k is the proportionality constant and n is the release exponent, concerning the mechanism of DOX release. For spherical micelles, if n is less than 0.43, the release was managed by Fickian diffusion basically. If n is more than 0.85, the release was governed by case-II transport, which is a swelling controlled method. If n has a value between 0.43 and 0.85, the DOX release behavior can be considered as the anomalous transport, which is the superposition of the above two circumstances.

On the basis of the equation, the plots of log (M_t / M_∞) against log t for DOX in mPEG-SS-St and mPEG-SeSe-St micelles with or without 10 mM GSH were displayed in Fig. 8, which showed that the Ritger and Peppas's equation was adapted to *in vitro* DOX release of mPEG-SS-St and mPEG-SeSe-St micelles because of the good linearity. The values of n for mPEG-SS-St and mPEG-SeSe-St micelles without GSH (0.24 and 0.26, respectively) were much less than 0.43, indicating that the release was Fickian diffusion chiefly. The value of n for mPEG-SS-St with 10 mM GSH (0.42) was close but still less than 0.43, suggesting a diffusion-controlled DOX release mechanism. The value of n for mPEG-SeSe-St with 10 mM GSH (0.48) was more than 0.43, illustrating the release was anomalous transport, which was combination the diffusion-controlled and the swelling-controlled DOX release mechanism. These results also indicated the rapid cleavage of diselenide linkages from mPEG-SeSe-St DOX-loaded micelles influenced the DOX release mechanism notably.

Intracellular drug release of DOX-loaded micelles

The cellular uptake and intracellular release behaviors of DOX loaded mPEG-SeSe-St micelles were investigated with mice TC1 lung cancer cells by confocal laser scanning microscopy (CLSM). Fig. 9 showed the CLSM images of TC1 cells incubated with DOX-loaded mPEG-SeSe-St micelles for 4, 12 and 24 h, respectively. Hydrophilic drug DOX•HCl and mPEG-SeSe-St micelles without DOX were used as the control. The dose of DOX was 15 μg/mL and the nuclei of the cells were dyed blue. After only 4 h of incubation with DOX-loaded mPEG-SeSe-St

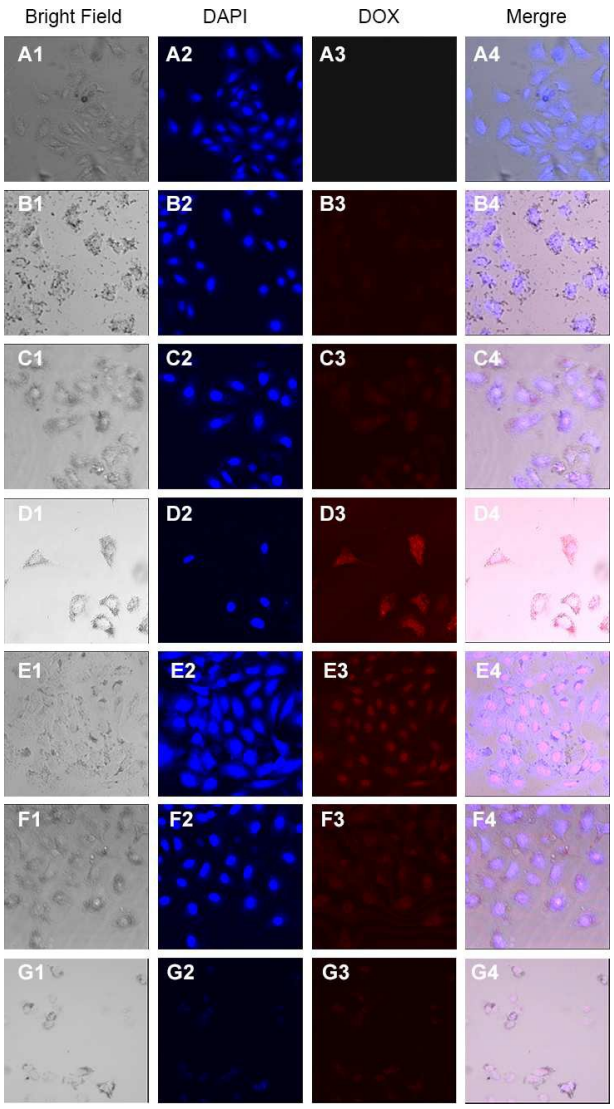

Fig. 9 The confocal laser scanning microscopy of mPEG-SeSe-St micelles incubated with mice TC1 lung cancer cells. (A) blank micelles for 4 h; DOX loaded micelles for (B)4 h, (C) 12 h, (D) 24 h; DOX•HCl for (E)4 h, (F) 12 h, (G) 24 h. The photographs from left to right are the images of bright field, stained nuclei, DOX and Merge.

micelles, feeble fluorescence could be visibly observed in cell cytoplasm and nuclei, testifying the cellular uptake of DOX/mPEG-SeSe-St occurred efficaciously. After 12 h, an evident fluorescence intensity was observed. When the incubation time was prolonged to 24 h, the strong red fluorescence was observed in cytoplasm and nuclei. However, strong red fluorescence was observed in the first 4 h incubation for the TC1 cells administrated with DOX•HCl. The longer incubation time (12 h, 24 h) contributed to weaker DOX fluorescence, which was opposite to the cells incubated with DOX-loaded mPEG-SeSe-St micelles under the same conditions. The reason might well because Free DOX was internalized into cells by diffusion, and it circulated from the medium to cytoplasm and then to nuclei rapidly, thus evident red fluorescence was found in both cytoplasm and nuclei after treatment with the cells for the first 4 h. With increasing incubation time, DOX was consumed, thus the fluorescence strength was weakened.[55] However, DOX-loaded micelles were slowly internalized into tumor cells by endocytosis into the cytoplasm. Endocytosis was a relatively slow process than diffusion. Owe to the EPR effect, the plasma membrane first invaginated and then formed a distinct intracellular compartment.[58] After escaped the endocytic vesicles (endosomes), the intracellular GSH concentration should fast trigger the degradation of the diselenide, resulting in intracellular release of DOX from mPEG-SeSe-St micelles and succedent localization of DOX in the cell nucleus. mPEG-SeSe-St micelles offer an effectual and safe platform with some unique characteristics, including increasing the aqueous solubility , prolonging the circulation time of DOX, minimizing systemic side effects and strengthening the impactful buildup at the tumor site by EPR effect. The cancer therapy need rapid and as complete as possible drug release after the micelles reach the pathological site in order to improve the therapeutic efficacy and minimize the probability of drug resistance.[28] Therefore, the trapped DOX in mPEG-SeSe-St micelles released was more favorable than Free DOX by diffusion.

Conclusions

In this work, a new kind of amphiphilic mPEG-SeSe-St nanocarriers was successfully synthesized by efficiently introducing mPEG grafted onto starch bones via functionalized diselenide bonds. Above the CAC, 0.049 mg/mL, the mPEG-SeSe-St self-assembled to form colloidally steady micellar aggregates having diselenide bonds at the mPEG/starch interface. Meanwhile, due to the intelligent linkage in the conjugates, the mPEG-SeSe-St micelles were bestowed with superb redox-sensitivity by size and morphology changes under low concentration of H_2O_2 (0.1% (v/v)) or GSH (1 mM). Furthermore, the micelles can readily encapsulate DOX and the *in vitro* drug release profiles revealed that only 45% of the loaded DOX from mPEG-SS-St micelles was released at 22 h with 10 mM GSH, while up to about 70% of the loaded DOX from mPEG-SeSe-St micelles could be rapidly released in the same period. These results, combined with intracellular release of DOX into TC1 Lung cancer cells confirmed by CLSM and MTT viability, suggested that the novel kind of amphiphilic mPEG-SeSe-St micelles had an outstanding redox-response and an excellent application potential in drug delivery.

Acknowledgements

The authors gratefully acknowledge the financial support of the National Natural Science Foundation of China (grant no.51273086, 51473072) and Special Doctorial Program Fund from the Ministry of Education of China (grant no. 20130211110017).

Notes and references

1. M. L. Adams, A. Lavasanifar and G. S. Kwon, *Journal of pharmaceutical sciences*, 2003, **92**, 1343-1355.

2. M.-C. Jones and J.-C. Leroux, *European journal of pharmaceutics and biopharmaceutics*, 1999, **48**, 101-111.
3. A. Rösler, G. W. Vandermeulen and H.-A. Klok, *Advanced Drug Delivery Reviews*, 2012, **64**, 270-279.
4. K. Kazunori, Y. Masayuki, O. Teruo and S. Yasuhisa, *Journal of Controlled Release*, 1993, **24**, 119-132.
5. G. Riess, *Progress in Polymer Science*, 2003, **28**, 1107-1170.
6. K. H. Min, H. J. Lee, K. Kim, I. C. Kwon, S. Y. Jeong and S. C. Lee, *Biomaterials*, 2012, **33**, 5788-5797.
7. C. Allen, J. Han, Y. Yu, D. Maysinger and A. Eisenberg, *Journal of Controlled Release*, 2000, **63**, 275-286.
8. C. Allen, A. Eisenberg, J. Mrsic and D. Maysinger, *Drug Delivery*, 2000, **7**, 139-145.
9. Y. Nagasaki, T. Okada, C. Scholz, M. Iijima, M. Kato and K. Kataoka, *Macromolecules*, 1998, **31**, 1473-1479.
10. H. Arimura, Y. Ohya and T. Ouchi, *Biomacromolecules*, 2005, **6**, 720-725.
11. J.-Z. Du, D.-P. Chen, Y.-C. Wang, C.-S. Xiao, Y.-J. Lu, J. Wang and G.-Z. Zhang, *Biomacromolecules*, 2006, **7**, 1898-1903.
12. H. R. Allcock, E. S. Powell, Y. Chang and C. Kim, *Macromolecules*, 2004, **37**, 7163-7167.
13. A. Zhang, Z. Zhang, F. Shi, J. Ding, C. Xiao, X. Zhuang, C. He, L. Chen and X. Chen, *Soft Matter*, 2013, **9**, 2224-2233.
14. Y. L. Li, L. Zhu, Z. Liu, R. Cheng, F. Meng, J. H. Cui, S. J. Ji and Z. Zhong, *Angewandte Chemie International Edition*, 2009, **48**, 9914-9918.
15. F. Meng, W. E. Hennink and Z. Zhong, *Biomaterials*, 2009, **30**, 2180-2198.
16. G. K. Balendiran, R. Dabur and D. Fraser, *Cell biochemistry and function*, 2004, **22**, 343-352.
17. S. Dodig and I. Čepelak, *Acta pharmaceutica*, 2004, **54**, 261-276.
18. A. Stazi and B. Trinti, *Minerva medica*, 2008, **99**, 643-653.
19. C. F. Bortolatto, S. O. Heck, B. M. Gai, V. A. Zborowski, J. S. Neto and C. W. Nogueira, *Psychopharmacology*, 2015, 1-11.
20. J. Beld, K. J. Woycechowsky and D. Hilvert, *Biochemistry*, 2007, **46**, 5382-5390.
21. H. Xu, W. Cao and X. Zhang, *Accounts of chemical research*, 2013, **46**, 1647-1658.
22. W. Li, P. Zhang, K. Zheng, Q. Hu and Y. Wang, *Journal of Materials Chemistry B*, 2013, **1**, 6418-6426.
23. P. Han, S. Li, W. Cao, Y. Li, Z. Sun, Z. Wang and H. Xu, *Journal of Materials Chemistry B*, 2013, **1**, 740-743.
24. W. Cao, X. Zhang, X. Miao, Z. Yang and H. Xu, *Angewandte Chemie*, 2013, **125**, 6353-6357.
25. H. Ren, Y. Wu, Y. Li, W. Cao, Z. Sun, H. Xu and X. Zhang, *Small*, 2013, **9**, 3981-3986.
26. N. Ma, H. Xu, L. An, J. Li, Z. Sun and X. Zhang, *Langmuir : the ACS journal of surfaces and colloids*, 2011, **27**, 5874-5878.
27. N. Ma, Y. Li, H. Xu, Z. Wang and X. Zhang, *Journal of the American Chemical Society*, 2009, **132**, 442-443.
28. T. Sun, Y. Jin, R. Qi, S. Peng and B. Fan, *Polymer Chemistry*, 2013, **4**, 4017-4023.
29. L. Meng, W. Huang, D. Wang, X. Huang, X. Zhu and D. Yan, *Biomacromolecules*, 2013, **14**, 2601-2610.
30. Y. Wang, Y. Liu, Y. Liu, Y. Wang, J. Wu, R. Li, J. Yang and N. Zhang, *Polymer Chemistry*, 2014, **5**, 423-432.
31. Y. Hu, X. He, L. Lei, S. Liang, G. Qiu and X. Hu, *Carbohydrate polymers*, 2008, **74**, 220-227.
32. P. Dandekar, R. Jain, T. Stauner, B. Loretz, M. Koch, G. Wenz and C. M. Lehr, *Macromolecular bioscience*, 2012, **12**, 184-194.
33. E. R. Balmayor, E. Baran, H. S. Azevedo and R. Reis, *Carbohydrate polymers*, 2012, **87**, 32-39.
34. H. Yamada, B. Loretz and C.-M. Lehr, *Biomacromolecules*, 2014, **15**, 1753-1761.
35. H. Hata, H. Matsuzaki, I. Sanada and K. Takatsuk, *Japanese journal of clinical oncology*, 1990, **20**, 246-251.
36. J. Joseph, S. Viney, P. Beck, C. Strange, S. A. Sahn and G. Basran, *CHEST Journal*, 1992, **102**, 1455-1459.
37. A. Zhang, Z. Zhang, F. Shi, C. Xiao, J. Ding, X. Zhuang, C. He, L. Chen and X. Chen, *Macromolecular bioscience*, 2013, **13**, 1249-1258.
38. M. Santander-Ortega, T. Stauner, B. Loretz, J. Ortega-Vinuesa, D. Bastos-González, G. Wenz, U. Schaefer and C. Lehr, *Journal of Controlled Release*, 2010, **141**, 85-92.
39. Y. Tan, K. Xu, Y. Li, S. Sun and P. Wang, *Chem. Commun.*, 2010, **46**, 4523-4525.
40. Y. H. Bae and K. Park, *Journal of Controlled Release*, 2011, **153**, 198.
41. O. C. Farokhzad and R. Langer, *ACS nano*, 2009, **3**, 16-20.
42. A. Prokop and J. M. Davidson, *Journal of pharmaceutical sciences*, 2008, **97**, 3518-3590.
43. O. Aronov, A. T. Horowitz, A. Gabizon and D. Gibson, *Bioconjugate chemistry*, 2003, **14**, 563-574.
44. T. Koch, E. Suenson, U. Henriksen and O. Buchardt, *Bioconjugate chemistry*, 1990, **1**, 296-304.
45. H. Liu, D. Chaudhary, S.-i. Yusa and M. O. Tadé, *Carbohydrate polymers*, 2011, **83**, 1591-1597.
46. N. W. Cheetham and L. Tao, *Carbohydrate polymers*, 1998, **36**, 277-284.
47. Y. Wang and S. M. Grayson, *Advanced Drug Delivery Reviews*, 2012, **64**, 852-865.
48. Y. Dong, Y. Jin and D. Wei, *Polymer international*, 2007, **56**, 14-21.
49. H. Zhou, W. Yu, X. Guo, X. Liu, N. Li, Y. Zhang and X. Ma, *Biomacromolecules*, 2010, **11**, 3480-3486.
50. H.-W. Lu, L.-M. Zhang, C. Wang and R.-F. Chen, *Carbohydrate polymers*, 2011, **83**, 1499-1506.
51. W. Y. Seow, J. M. Xue and Y.-Y. Yang, *Biomaterials*, 2007, **28**, 1730-1740.
52. S. Taurin, H. Nehoff and K. Greish, *Journal of Controlled Release*, 2012, **164**, 265-275.
53. L. Zhang, Y. Li and C. Y. Jimmy, *Journal of Materials Chemistry B*, 2014, **2**, 452-470.
54. V. T. Huynh, P. de Souza and M. H. Stenzel, *Macromolecules*, 2011, **44**, 7888-7900.
55. J. Chang, Y. Li, G. Wang, B. He and Z. Gu, *Nanoscale*, 2013, **5**, 813-820.
56. P. L. Ritger and N. A. Peppas, *Journal of Controlled Release*, 1987, **5**, 37-42.
57. L. Wei, C. Cai, J. Lin and T. Chen, *Biomaterials*, 2009, **30**, 2606-2613.

58. H. Zhang, F. Li, J. Yi, C. Gu, L. Fan, Y. Qiao, Y. Tao, C. Cheng and H. Wu, *European Journal of Pharmaceutical Sciences*, 2011, **42**, 517-526.

The new diselenide-linked mPEGylated starch amphiphilic micelles was developed, which could be disrupted in the presence of 0.1% (v/v) H_2O_2 or 1 mM GSH.